A Study on Nonlinear Finite Element Analysis of Reinforced Concrete Plates

Rifat SEZER[1],Muhammed TEKIN[2]

Abstract - In this study, Finite Elements Method was used for the nonlinear analysis of reinforced concrete plates under gradually loading conditions beginning from zero load to failure load. Layered Composite Material Model was used for the modeling of reinforced concrete plates. The principles of this approach is given in "layered composites mechanics" that it was successfully applied for the nonlinear analysis of reinforced concrete plates. This approach differs from the other approaches by considering the effect of tensile rigidity of the concrete between cracks and by using a criterion based on the crack energy concept together with the consideration of the effect of finite element network dimension. Load-displacement relationships were determined according to the Layered Composite Material Approach. The results of the analyses were compared and found to be in agreement with the experimental results and the results of past studies. A computer program prepared with Fortran PowerStation 4.0 programming language was used for the determination of this study's results.

Index Terms - Finite element method, reinforced concrete, nonlinear analysis, Layered Composites.

1 INTRODUCTION

The analysis of reinforced concrete structures by using an analytical method is an advanced but complex process due to the following reasons; 1- Reinforced concrete structures are formed by the combination of two different materials, i.e. concrete and steel, 2- The effects due to tensile crack, biaxial rigidity, nonlinear behavior of concrete and decrease in strain, 3- Non-adherence and aggregate locking between concrete and reinforcement bars, etc. In general, for the analysis of reinforced concrete plates and beams with Finite Elements Method, two different approaches are used; a- Modified Rigidity Approach, b-Layered Approach (also used in this study).

Choi and Kwak [1] investigated the effect of finite element mesh dimension on the nonlinear analysis of reinforced concrete structures. Hu and Schnobrich [2] carried out the nonlinear analysis of reinforced concrete plates and shells under gradually increasing loads by the aid of finite elements method. Sathurappan et all [3] studied the nonlinear analysis of the reinforced and prestressed concrete plates and shells by using the finite elements method. Sezer [4] investigated the nonlinear analysis of reinforced concrete plates according to the finite elements method. Özer [5] described the nonlinear analysis of structural systems in detail according to various methods. Zhang et all [6] performed the nonlinear analysis of the reinforced concrete cylindrical shells and plates modeled with layered rectangular elements by using finite elements method. Sezer and Tekin [7] investigated nonlinear finite element analysis of reinforced concrete plates modeled by layered composites. Mamede et all [8] studied experimental and parametric 3D nonlinear finite element analysis on punching of flat slabs with orthogonal reinforcement. Xiaodan and Zhang [9] searched nonlinear finite element analyses of FRP-strengthened reinforced concrete slabs using a new layered composite plate element.

Thiagarajan et all [10] investigated experimental and finite element analysis of doubly reinforced concrete slabs subjected to blast loads. Xiaodan et all [11] studied two new composite plate elements with bond–slip effect for nonlinear finite element analyses of FRP-strengthened concrete slabs.

(1) Assoc. Prof. Dr. Rifat Sezer, Selçuk University, Engineering Faculty, Civil Engineering Department, Konya, Turkey, e-mail: rsezer@selcuk.edu.tr

(2) Prof. Dr. Muhammed Tekin, Gelisim University, Engineering and Architecture Faculty, Civil Engineering Department, Istanbul, Turkey, e-mail: mtekin@gelisim.edu.tr

Genikomsou and Polak [12] investigated finite element analysis of punching shear of concrete slabs using damaged plasticity model in ABAQUS. Escudero et all [13] researched a laminated structural finite element for the behavior of large non-linear reinforced concrete structures. Razaqpur and Esfandiari [14] studied nonlinear finite element analysis of strength and durability of reinforced concrete and composite structures. Shu et all [15] investigated prediction of punching behaviour of RC slabs using continuum non-linear finite element analysis.

2 MATERIAL PROPERTIES AND ASSUMPTIONS

In order to formulize the basic relationships of a reinforced concrete member of a layer, the following simplified assumptions were accepted; a) Concrete and steel inside the member are divided into some imaginary layers (Figure 1), b) The bending of plates occurs according to the Mindlin Plate Theory, c) Steel reinforcement carries only the uniaxial stress, 4) There is perfect adherence between steel and concrete [1], [4], [7].

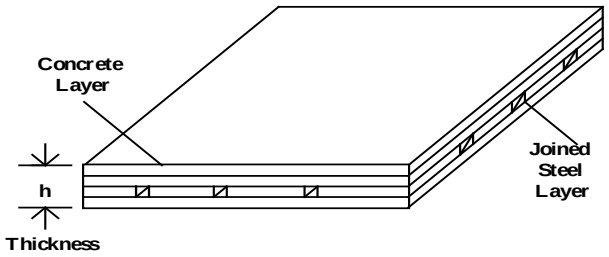

Figure 1. Layered system

2.1 Reinforcement

Reinforcement steel with σ_y yield stress was assumed to be a material presenting linear strain hardening (Figure 2). Stress-strain relationship of the reinforcement can be expressed as in the following by referencing local axes selected parallel and perpendicular to the direction of the reinforcement.

$$\begin{Bmatrix} \sigma_1 \\ \sigma_2 \\ \tau_{12} \end{Bmatrix} = \begin{bmatrix} E_{s1} & 0 & 0 \\ 0 & 0 & 0 \\ 0 & 0 & 0 \end{bmatrix} \begin{Bmatrix} \varepsilon_1 \\ \varepsilon_2 \\ \gamma_{12} \end{Bmatrix}$$

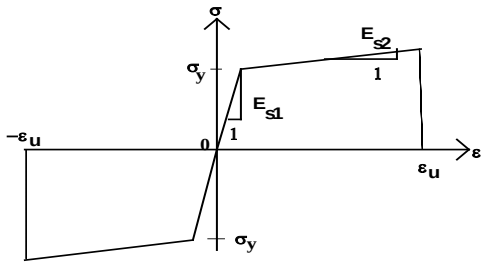

Figure 2. Idealized uniaxial stress-strain relationship of steel

Here, E_{s1} is the first modulus of elasticity of steel. When steel yields, the second modulus of elasticity E_{s2} is used in place of E_{s1} [1], [4], [7].

2.2 Concrete

As seen in Figure 3, f_{eq} is the end-point stress on the right. Concrete under biaxial stress was assumed to behave linearly elastic at the tension zone. In this case, the stress linearly decreases by

equal amount increase in the uniaxial strain. If concrete is at the compression zone, it will be accepted as elasto-plastic hardening model.

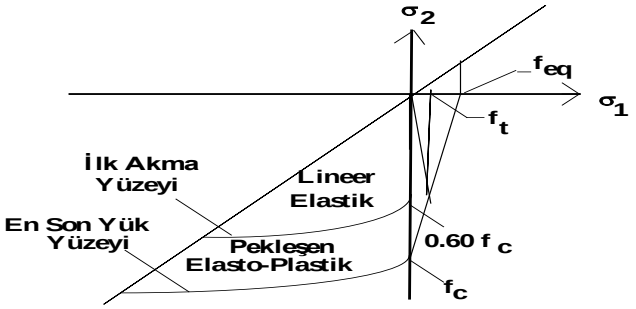

Figure 3. Biaxial strength envelope of concrete

$$F = [\ (\sigma_1 + \sigma_2)^2 / (\sigma_2 + 3.65\sigma_1)\ ] - Af_c = 0 \qquad (2)$$

Here, σ_1 and σ_2 are the principal stresses; f_c represents the uniaxial compression strength and A is the parameter symbolizing plastic yielding from initial yielding surface (A=0.6) to final loading surface (A=1.0). In order to check the cracking condition of concrete continuously, similar to the yielding surface of Equation 2, a crack surface (Figure 4) was determined using strain terms and defined by the following equation.

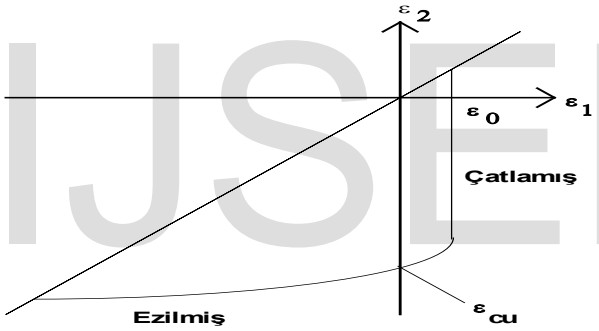

Figure 4. Cracking Surface of Concrete

$$C = [\ (\varepsilon_1 + \varepsilon_2)^2 / (\varepsilon_2 + 3.65\varepsilon_1)\ ] - \varepsilon_{cu} = 0 \qquad (3)$$

Here, ε_1 and ε_2 are the principal strains, and ε_{cu} is the maximum strain of concrete under compression [1], [4], [7].

2.3 Rigidity of Cracked Concrete

When principal tensile strain is exceeded for a few (Figure 5), cracks perpendicular to the principal stress will develop. Shear modulus should be reduced by cracking. However, intending to determine an effective shear modulus is more complex besides determining the lever effect and aggregate locking effects.

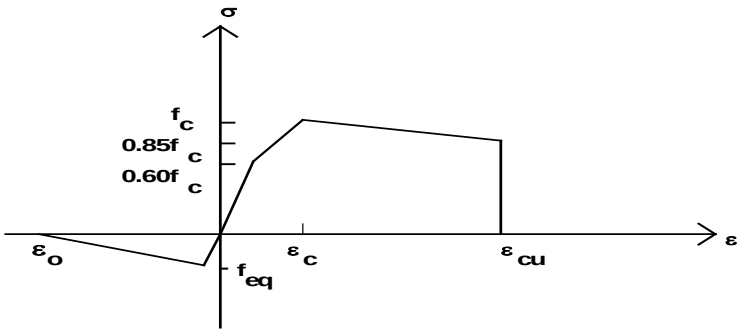

Figure 5. Idealized Uniaxial Stress-Strain Relationship of Concrete

Therefore, the value of cracked shear modulus was assumed to be continuously constant also after the cracking event; i.e in Equation (4) λ = 0.4. Then the cracked rigidity will be accepted as in the following;

$$\begin{Bmatrix}\sigma_1\\ \sigma_2\\ \tau_{12}\end{Bmatrix}=\frac{1}{1-\nu^2}\begin{bmatrix}E_1 & 0 & 0\\ 0 & 0 & 0\\ 0 & 0 & \lambda\frac{1-\nu}{2}G\end{bmatrix}\begin{Bmatrix}\varepsilon_1\\ \varepsilon_2\\ \gamma_{12}\end{Bmatrix} \qquad (4)$$

Here, axes 1 and 2 are respectively parallel and perpendicular to the cracks. G and λ are the shear modulus of uncracked concrete and shear constant of the cracked concrete, respectively. If the cracking of concrete occurs biaxially, then E_1 will be taken as zero [1], [4], [7].

2.4 Tensile Rigidity Effect

The increase in tensile rigidity of concrete can be provided by using the stress-strain relationship of the decreasing section at the tensile zone. On the other hand, the nonlinear form of the cracking model should be used in order to estimate the displacements of the structure more precisely. About this subject, stress-controlled cracking model was firstly used by Rashid (Choi, Kwak, 1990) for the numerical analysis of the reinforced concrete structures. However, this model has some negative sides such as being independent from finite element network dimensions, etc. Many researchers most of which were interested in cracking mechanics suggested the "cracked band theory", the simplest model of fictive cracking models on planar concrete panels. Two basic assumptions of this model are; a. the deformation inside the band is uniform, b. the width of the cracking zone has a certain b value directly proportional to three times of the maximum aggregate size (3 x 25.4mm). Then, the equation for finding ε_0 is given in the following.

$$\varepsilon_0=\frac{2G_f}{f_t b} \qquad (5)$$

This model can be successfully applied to the reinforced concrete problems, when relatively small finite element network dimension is used. However, Equation (5) will not be sufficient for the direct application of this model to the numerical analysis of reinforced concrete structures modeled with relatively large finite element network dimensions [1], [4], [7].

2.5 Applied Crack Model

A new criterion applicable to an extremely large finite element network dimension was used for the nonlinear analysis of the reinforced concrete structures.

2.6 Distribution of Microcracks

At first, in order to formulize the distribution of the microcracks of a member, an exponential function is given in the following (Figure 6).

$$f(x) = \alpha\, e^{\beta x} \qquad (6)$$

Here, α and β are specifiable constants. If the boundary conditions, i.e. f(0) = 1.0 and f(b/2)= 3/b are substituted in Equation (6), the following equation will be determined.

$$f(x) = e^{-2b \ln (b/3)\, x} \qquad (7)$$

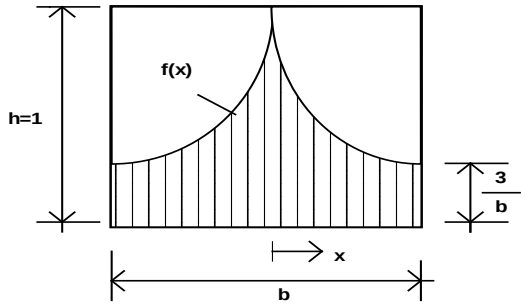

Figure 6. Assumed Distribution of Microcracks in a Member

Here, b is the width of the member. For the expressions of f(x) function defined in Equations (6) and (7), **1)** The distribution of microcracks has a symmetrical characteristic as shown in Figure 6, **2)** The typical dimension of microcrack at the end of the finite member network is 3/b. The second property proves that the microcrack distribution is uniform for the condition of a width less than 76 mm [1], [4], [7].

2.7 Cracking Energy

The stress-strain relationship and cracking energy of concrete are given in the following;

$$G_f = \frac{1}{2}\varepsilon_0 f_t \int_0^{b/2} f(x)dx2 \qquad (8)$$

Here, f_t is the tensile strength of concrete, ε_o is the strain at the end of the decreasing strain zone and G_f is the consumed cracking energy of a crack with unit length through the unit thickness. If G_f and f_t are known from measurements, then ε_o can be calculated as in the following;

$$\varepsilon_0 = \frac{G_f}{f_t \int_0^{b/2} f(x)dx} \qquad (9)$$

If finite element network dimension is changed, E_o can be calculated by using Equation (7). For f(x) = 1.0, the suggested criterion in Equations (5) and (9) gives the same result, i.e. finite element network dimension is equal to or less than 76 mm. When finite element network dimension is greater than 76 mm, the microcracks distribution of the member should be accepted according to the f(x) function in Equation (7), as applied in most of the practical conditions [1], [4], [7].

3 REINFORCED CONCRETE APPLICATION OF FINITE ELEMENT METHOD

As shown in Figure 7, a typical finite element is divided into imaginary concrete and composite (formed with concrete and steel) layers. It is assumed that the displacement area of the member is continuous and there are no gaps between layers. The material properties of each layer may differ but they present a homogeneous structure through the thickness of the layer. Then, the integration volume involving the material properties can be written as in the following;

$$\int [B]^T [D][B] dv = \sum \int_{i=1}^{n_k} {}_v [B]^T [D_k]_i [B] dV + \sum \int_{j=1}^{n_c} {}_v [B]^T [D_c]_j [B] dV \qquad (10)$$

Here, $[D_k]_i$ and $[D_c]_i$ are the material matrices of the i^{th} composite layer and j^{th} concrete layer, and n_k and n_c are the number of composite and concrete layers respectively.

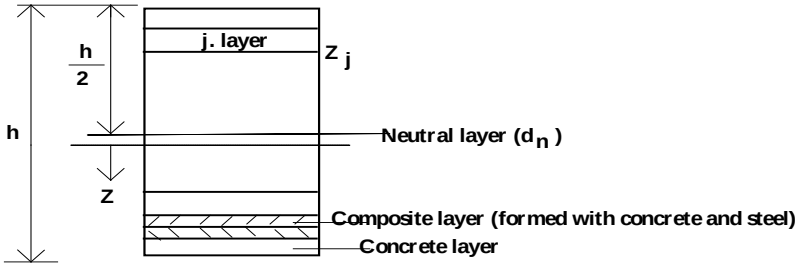

Figure 7. A layered cross-section

The displacement area based on Mindlin Hypothesis can be defined in matrix form as in the following;

$$\{d\} = \begin{Bmatrix} w \\ \theta_x \\ \theta_y \end{Bmatrix} = \sum_{j=1}^{n} \begin{bmatrix} N_j & 0 & 0 \\ 0 & N_j & 0 \\ 0 & 0 & N_j \end{bmatrix} \begin{Bmatrix} w \\ \theta_x \\ \theta_y \end{Bmatrix}_j \qquad (11)$$

where n is the number of nodes and N_j is the interpolation function. The relationship between strain and displacements can be written as;

$$\begin{Bmatrix} \varepsilon_x \\ \varepsilon_y \\ \gamma_{xy} \end{Bmatrix} = \begin{bmatrix} 0 & -\frac{\partial N}{\partial x} & 0 \\ 0 & 0 & -\frac{\partial N}{\partial y} \\ 0 & -\frac{\partial N}{\partial x} & -\frac{\partial N}{\partial y} \end{bmatrix} \begin{Bmatrix} w \\ \theta_x \\ \theta_y \end{Bmatrix} \qquad (12)$$

or

$$\{\varepsilon_p\} = [B_p]\{u\} \qquad (13)$$

The relationship between transversal shear strains and displacements can be given as;

$$\begin{Bmatrix} \gamma_{xz} \\ \gamma_{yz} \end{Bmatrix} = \begin{bmatrix} -\frac{\partial N}{\partial y} & -N & 0 \\ -\frac{\partial N}{\partial y} & 0 & -N \end{bmatrix} \begin{Bmatrix} w \\ \theta_x \\ \theta_y \end{Bmatrix} \qquad (14)$$

or

$$\{\varepsilon_t\} = [B_t]\{u\} \qquad (15)$$

After substituting the sub-equations of Equations (13) and (15) into Equation (10), and rearranging the material matrix, the member rigidity matrix can be written as in the following;

$$[K] = \int_v [B_p]^T [D_p] [B_p] \, dV + \int_v [B_t]^T [D_t] [B_t] \, dV \qquad (16)$$

Here, $[D_p]$ and $[D_t]$ given in Equation (17) are the flexural and shear sections of the material matrix, respectively (Choi, Kwak, 1990).

$$D_{pij} = \sum_{k=1}^{N} (\bar{Q_{ij}})_k (h_k z_k + \frac{h^3{}_k}{12}), \qquad [D_t] = \frac{Ehk}{2(1+\nu)} \begin{bmatrix} 1 & 0 \\ 0 & 1 \end{bmatrix} \qquad (17)$$

where z_k is the height from the central surface to the center of the k^{th} layer, h_k is the thickness of the layer, (Q^-_{ij}) represents the flexural rigidities of the k^{th} layer which can be calculated by Equation (18) for the orthotropic plates. k (in the second equation) is the shear correction factor having the value of 5/6, E is the modulus of elasticity and ν is the Poisson's ratio.

$$\left(Q^-_{11}\right)_k = \frac{E^k_1}{1-\nu^k_{12}\nu^k_{21}}\ , \quad \left(Q^-_{12}\right)_k = \frac{\nu^k_{12}E^k_1}{1-\nu^k_{12}\nu^k_{21}}\ , \quad \left(Q^-_{22}\right)_k = \frac{E^k_2}{1-\nu^k_{12}\nu^k_{21}} \tag{18}$$

$$\left(Q^-_{16}\right)_k = 0\ , \qquad \left(Q^-_{26}\right)_k = 0\ , \qquad \left(Q^-_{66}\right)_k = G^k_{12}$$

Here, G^k_{12} is the shear modulus parallel to surface 1. The calculation procedure of node displacement parameters and each layer's strain members determined by Equations (13) and (15) are given in the following for both concrete and composite layers.

$$\{\varepsilon_c\}_j = \begin{Bmatrix} \varepsilon_{xj} = (-d_{nx} + 0.5h + z_j)\dfrac{\partial\theta_x}{\partial x} \\ \varepsilon_{yj} = (-d_{ny} + 0.5h + z_j)\dfrac{\partial\theta_y}{\partial y} \\ \gamma_{xyj} = (-d_{nxy} + 0.5h + z_j)\left(\dfrac{\partial\theta_x}{\partial x} + \dfrac{\partial\theta_y}{\partial y}\right) \\ \gamma_{xzj} = \dfrac{\partial w}{\partial x} - \theta_x \\ \gamma_{xzj} = \dfrac{\partial w}{\partial x} - \theta_x \end{Bmatrix}, \quad \{\varepsilon_s\}_i = \begin{Bmatrix} \varepsilon_{xi} = (d_x - d_{nx})\dfrac{\partial\theta x}{\partial x} \\ \varepsilon_{yi} = (d_y - d_{ny})\dfrac{\partial\theta y}{\partial y} \end{Bmatrix} \tag{20}$$

Here, d_{nx}, d_{ny} and d_{nxy} given to prevent the development of unwanted forces on the plane represent the neutral axis depths (Figure 7) that can be calculated under the condition of $\int\sigma_x\, dz = \int\sigma_y\, dz = \int\tau_{xy}\, dz = 0$; where z is the depth measured from the central surface (Figure 7). Additionally, the simplified assumptions used here are; 1- Shear modulus G is constant through the depth, 2- d_{nxy} value is nearly equal to h/2 where h is the thickness of the member, 3- d_x and d_y are the useful heights in x and y directions, 4- z_j is the height measured from the central surface to the center of the concrete layer (Figure 7).

$$\{\sigma_c\}_i = \left[Q^-\right]_{ki}\{\varepsilon_c\}_i \tag{21}$$

or

$$\begin{Bmatrix}\sigma_x \\ \sigma_y \\ \tau_{xy}\end{Bmatrix}_{cj} = \begin{bmatrix} Q^-_{11} & Q^-_{12} & 0 \\ Q^-_{12} & Q^-_{22} & 0 \\ 0 & 0 & Q^-_{66}\end{bmatrix}\begin{Bmatrix}\varepsilon_x \\ \varepsilon_y \\ \gamma_{xy}\end{Bmatrix}_{cj} \tag{22}$$

The stress-strain relationship in the local axes parallel and perpendicular to the reinforcement bar can be written as in Equation (23) by using Equation (1).

$$\{\sigma_s\}_i = \left[Q^-\right]_{ki}\{\varepsilon_s\}_i \tag{23}$$

Here, $\{\sigma_s\}_i$ ve $\{\varepsilon_s\}_i$ represent the stress and strain values at the center of the i^{th} steel layer and $\{\sigma_c\}_j$ and $\{\varepsilon_c\}_j$ represent the stress and strain values at the center of the j^{th} concrete layer, respectively (Sezer and Tekin, 2011). In nonlinear problems, the calculated stresses do not agree with the real stresses due to unbalanced node forces. The equivalent node forces can be determined statically in the equivalent stress zone by Equation (24).

$$\{R\}_{equivalent} = \int_v [B]^T\{\sigma\}dV = \int_v [B]^T\{\sigma_p\}dV + \int_v [B]^T\{\sigma_t\}dV \tag{24}$$

Unbalanced node forces can be calculated by using Equation (25).

$$\{R\}_{unbalanced} = \{R\}_{applied} = \{R\}_{equivalent} \quad (25)$$

In the solution, a load increase was applied to determine the unbalanced node forces that were iteratively recalculated to approach the convergence tolerance [4], [7].

4 NUMERICAL EXAMPLE

A two-way slab supported by its four edges (Figure 8) and solved in the literature was resolved by the aid of the newly developed computer program. The slab subjected to uniform load has a square shape with 1200 mm side length, 75 mm thickness, and the ratios of reinforcement in isotropic network shape are ρ_x=0.00548 and ρ_y=0.00629. The selected material properties are; concrete's Poisson's ratio ν_c = 0.15, tensile strength f_{ctk} =3.5 N/mm², compression strength f_{ck} =36.8 N/mm², modulus of elasticity E_c=34580 N/mm², cracking energy G_f = 0.09 N/mm, and the number of concrete layers is n_c= 8. The yield strength and modulus of elasticity of steel are respectively f_{yk} = 400 N/mm² and E_s=2.10⁵ N/mm². The useful height are d_x=61 mm and d_y=53 mm [3], [4], [7].

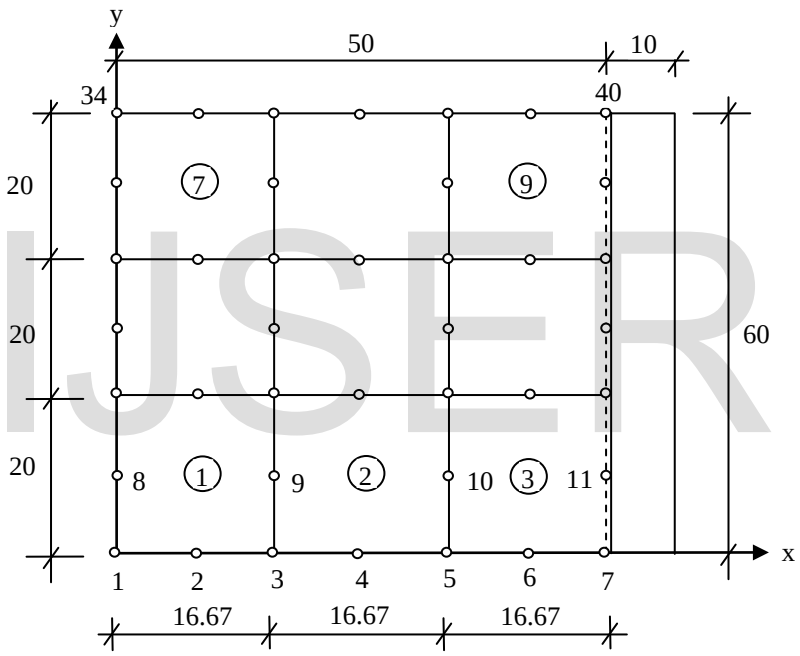

Figure 8. One-way slab supported by its two edges (all dimensions cm)

The finite element network used in this study is given in Figure 8. The displacement amounts at node 1 with respect to load increases were determined in agreement with the results of literature. The load-displacement values are given in Table 1. The graphical representation of load-displacement relationship at node 1 is given in Figure 9. The displacement at node 1 can be approximately calculated by making interpolation with the displacements of the adjacent nodes.

Table 1. Load-displacement values at node 1 in Figure 8

Laod No	Load (kN)	Displacement (mm)		
		Experiment [3]	Sathurappan [3]	This study
1	20	0.23	0.21	0.27
2	40	0.45	0.23	0.80
3	60	1.82	1.36	1.83
4	80	3.40	2.73	2.44

5	100	6.14	6.36	7.53
6	120	12.72	13.86	12.70

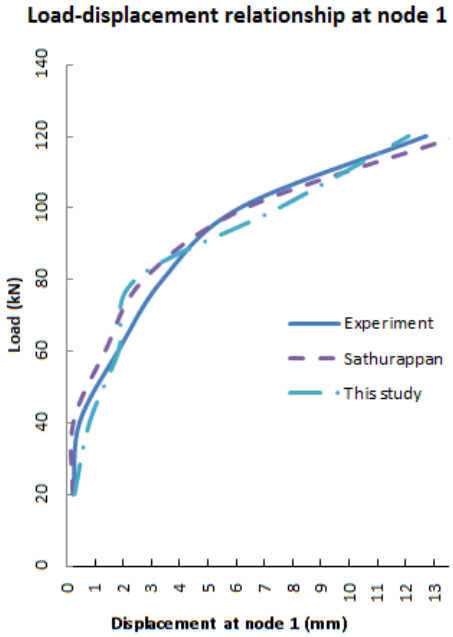

Figure 9. Load-displacement relationship at node 1 in Figure 8

5 CONCLUSION

In this study, isoparametric members with four, eight and nine nodes were used to perform the finite element modeling by using Layered Approach. The reinforced concrete plate (Figure 8) supported by its four edges was solved with a newly developed finite element model program prepared with Fortran PowerStation 4.0 computer programming language. The results are compared with the results of literature for the same plate in Table 2. After comparing the results of this study with the results of literature and experimental study for the same subject, the results of this study were in agreement with the results of both literature and experimental study.

Table 2. The comparison of results determined by this study with the test results of literature (for the plate in Figure 8)

Average differences according to the test results of literature (%)	
Sathurappan [3]	This study
19.17	18.33

REFERENCES

[1] Choi, C.K., Kwak, H.G. "The effect of finite element mesh size in nonlinear analysis of reinforced concrete structures", *Comput. Struct.* Vol.36, No.5: 807-815, 1990. doi:10.1016/0045-7949(90)90151-Q.

[2] Hu, H.T., Schnobrich, W.C. "Nonlinear finite element analysis of reinforced concrete plates and shells under monotonic loading", *Comput. Struct.* Vol.38, No.5/6:637-651, 1991. doi:10.1016/0045-7949(91)90015-E.

[3] Sathurappan, G., Rajagopalan, N., Krishnamorthy, C.S. "Nonlinear finite element analysis of and prestressed concrete slabs with reinforcement (inclusive of prestresing steel) modeled

as discrete integral components", *Computer & Structures*, Vol.44, No.3, pp.575-584, 1992. doi:10.1016/0045-7949(92)90390-L.

[4] Sezer, R. "Nonlinear analysis of reinforced concrete plates by finite elements methods", Selcuk University, Graduate School of Natural and Applied Sciences, PhD, Konya, Turkey. 1995.

[5] E. Özer, E. "Nonlinear Analysis of Structures Systems", Technical University, Doctorate Lessons Notest, Istanbul, Turkey. 2006.

[6] Zhang Y.X., Bradford M.A., Gilbert R.I. "A layered cylindrical quadrilateral shell element for nonlinear analysis of RC plates structures", *Advances Engineering Software* 38: 488-500, 2007. http://dx.doi.org/10.1016/j.advengsoft.2006.09.017.

[7] Sezer, R., Tekin, M.D. "Nonlinear finite element analysis of reinforced concrete plates modeled by layered composites", *Scientific Research and Essays* 6 (15), 3281-3289, 2011. doi: 10.5897/SRE11.547.

[8] Mamede, N.F.S., Ramos, A.P., Faria, D.M.V. "Experimental and parametric 3D nonlinear finite element analysis on punching of flat slabs with orthogonal reinforcement." *Engineering Structures* 48: 442-457, 2013. http://dx.doi.org/10.1016/j. engstruct.2012.09.035.

[9] Xiaodan T., Zhang,Y.X.. (2014). "Nonlinear finite element analyses of FRP-strengthened reinforced concrete slabs using a new layered composite plate element." *Composite Structures* 114: 20-29, 2014. http://dx.doi.org/10.1016/ j.compstruct.2014.03.040.

[10] Thiagarajan, G., Kadambia, A.V., Robertb, S., Johnson, C.F. (2015). "Experimental and finite element analysis of doubly reinforced concrete slabs subjected to blast loads." *International Journal of Impact Engineering* 75: 162-173, 2015. http://dx.doi.org/10.1016/j.engstruct. 2012.09.035.

[11] Teng, Xiaodan, Y. X. Zhang, and Xiaoshan Lin. "Two new composite plate elements with bond–slip effect for nonlinear finite element analyses of FRP-strengthened concrete slabs." Computers & Structures 148: 35-44, 2015.

[12] Genikomsou, A.S., and Polak, M.A. "Finite element analysis of punching shear of concrete slabs using damaged plasticity model in ABAQUS." *Engineering Structures* 98: 38-48, 2015. http://dx.doi.org/10.1016/j.engstruct.2015.04.016.

[13] Escudero, C., Oller, S., Martinez, X., Barbat, A.H. "A laminated structural finite element for the behavior of large non-linear reinforced concrete structures." *Finite Elements in Analysis and Design* 119: 78-94, 2016. http://dx. doi.org/10.1016/j.finel.2016.06.001.

[14] Razaqpur, A.G., Isgor, O.B., Esfandiari, A. "Nonlinear finite element analysis of strength and durability of reinforced concrete and composite structures." *Engineering Structures* 123: 330–340, 2016. doi: http://dx.doi.org/ 10.20528/cjsmec.2015.09.030.

[15] Shu, J., Plos, M., Zandi, K., Johansson, M., Nilenius, F. "Prediction of punching behaviour of RC slabs using continuum non-linear FE analysis." *Engineering Structures* 125: 15-25, 2016. http://dx.doi.org/10.1016/j.engstruct.2016.06.044.